PHYSICAL REVIEW A VOLUME 35, NUMBER 1 JANUARY 1, 1987

Theory and phenomenology of growth oscillations in simple deterministic models

Zheming Cheng, Rachid Baiod, and Robert Savit
Physics Department, The University of Michigan, Ann Arbor, Michigan 48109
(Received 4 August 1986)

We study growth oscillations in a class of deterministic models of growth which may be regarded as mean-field-like approximations to certain more realistic stochastic models. We demonstrate that the general morphology of the stochastic and deterministic models are similar. We then show that growth oscillations produce a rich multiperiodic structure in the deterministic models, as they do in the related stochastic systems. In both cases the multiperiodic oscillations are due to an induced incommensuration between a fundamental length scale (in this case the lattice spacing) and a dynamical length scale (in this case, the average distance grown per time step). We show how to estimate the effects of the growth oscillations and how to solve the deterministic equations analytically. This solution leads to a series of approximations, successive terms of which include the effects of longer-wavelength contributions to the multiperiodic growth oscillations. Finally, we present a sequence of approximations, the first one of which is the deterministic model studied here, which approach the related stochastic models.

I. INTRODUCTION

It has recently been shown[1–3] that several models of kinetic growth processes possess a remarkable and unexpected feature, namely, the existence of oscillations in the propagation of the growing interface. These oscillations, which we refer to as "growth oscillations," seem to be quite an ubiquitous phenomenon, and can, generally, be expected in processes satisfying the following two conditions: (i) Growth takes place at a fairly well defined interface and (ii) the growth process is discrete, i.e., material agglomerates onto the growing cluster in packets or particles of finite size. As we have argued elsewhere,[2] having satisfied these conditions, the growing structure can generically be expected to develop a dynamically induced incommensuration. In the lattice models discussed in Ref. 2 (hereinafter referred to as I), and in the present paper, it is easy to see that the induced incommensuration is between two length scales. The first is the static small distance cutoff, which in these models is the lattice spacing. The second is a dynamically defined length scale, which in these models is the average distance which the growing interface moves in one time step. (Arguments for the existence of growth oscillations in nonlattice models were presented in I and are discussed briefly in the conclusions of the present paper.)

These oscillations have observable physical consequences and result in, among other things, interesting multiperiodic oscillations in the density and growth velocity of the cluster. In I, phenomenology of growth oscillations in a simple stochastic model of growth was studied in some detail. This model[4] (although differing in some important details) is a close cousin of the Broadbent, Hammersley, Leath, and Alexandrowicz algorithm for the generation of percolation clusters.[5] Paper I also contained an extensive qualitative discussion concerning the origin and generality of growth oscillations.

In this paper we wish to study growth oscillations further by turning our attention to a deterministic model of growth which has the form of a rather complicated iterative map, and which can be thought of as a kind of "mean-field" approximation to the stochastic model discussed in I. The clusters generated by the deterministic model studied in this paper exhibit both a morphology and growth oscillations which are qualitatively similar to those seen in the stochastically grown clusters of the model of paper I. However, we are able to make considerably more analytical and numerical progress on this deterministic model, and this has led to deeper insights into the nature of the growth oscillations phenomenon and its behavior in various circumstances. Furthermore, if we consider the model studied in this paper as a first approximation to the stochastic model of paper I, we are able to suggest a sequence of successively better approximations to the physically more realistic stochastic case. As we shall discuss below, this may be useful in trying to calculate the behavior of kinetic growth near a critical value of its control parameter, which corresponds to kinetically generated fractal aggregates.

The rest of this paper is organized as follows. In Sec. II we briefly review the stochastic model of paper I and demonstrate that our deterministic model is a mean-field-like approximation to it. Using a numerical solution of the deterministic map in two dimensions, we show that the stochastic and deterministic (mean-field) models have qualitatively similar morphologies. We then turn our attention to a construction of simple one-dimensional and quasi-one-dimensional deterministic models (a term which will be explained below) with which we will study various aspects of the growth. We discuss the way in which the structure of these simple deterministic maps changes when we change the initial conditions or dimensionality of the system. In Sec. III we present a detailed study of the one-dimensional deterministic maps constructed in Sec. II. For this realization of the model we present a variety of numerical and analytical results including (i) a series of

numerical solutions which exhibit density oscillations for various values of p, the control parameter, (ii) a procedure for obtaining an analytical solution of the deterministic problem. This analytic procedure also results in an approximation scheme for the density which can be thought of as an expansion, higher terms of which represent the contribution to the density of oscillations of successively longer periods, and (iii) a determination of the behavior of the growth when p is near p_c, the critical value of p at which growth is marginal. (p_c is the analogue of the value of the control parameter which, in a more realistic model of stochastic growth, would lead to the growth of a fractal-like structure.) We will show that in this case the density of the cluster falls off like an inverse power of x at $p=p_c$. Some of the results and methods presented in this section can be applied more generally, and we indicate when this is so.

In Sec. IV we discuss a larger class of related deterministic models. These models, although formally one-dimensional, also describe growth normal to a $(d-1)$-dimensional facet embedded in d dimension. We will show that for these models, there are two critical values of p at which the growth undergoes qualitative changes both in its morphology and in the nature of its oscillations. Roughly speaking, one of the critical values of p is associated with a faceting transition and the other with the analog of marginal fractal growth. Furthermore, in this section we will present a simple argument which will help to explain the multiperiodic nature of the growth oscillations and their qualitative dependence on p.

In Sec. V we will discuss the relationship between the stochastic and deterministic models further. In particular, we will describe a sequence of approximations which allows us to systematically approach the stochastic model. The first member of this sequence is just the deterministic model discussed in the earlier sections of this paper. Section VI consists of a summary, conclusions, and a catalog of interesting remaining problems, along with suggestions concerning their solution.

II. GENERAL FEATURES OF THE STOCHASTIC AND DETERMINISTIC MODELS

To describe the stochastic model of growth studied in Refs. 1, 2, and 4, consider a d-dimensional hypercubic lattice (usually, we will consider the case $d=2$) with some set of initially filled sites. For specificity, consider initial conditions consisting of a single seed particle at the origin of the lattice. (Other initial conditions will be discussed below.) In the first time step, fill each nearest neighbor site of the seed particle independently and stochastically with a probability p. Call the sites so filled the second generation. In the next time step fill the empty nearest neighbors of the second generation independently and stochastically with a probability p. Continue growing the cluster by testing, in the nth time step, all the nearest neighbors of the nth generation and filling each one with a probability p. This algorithm may be summarized by the following iterative equation:

$$S_{n+1}(x)=q_n(x)\left[1-\prod_y [1-S_n(y)]\right]\prod_{m=1}^{n}[1-S_m(x)] \tag{2.1}$$

with

$$\langle q_n(x)\rangle = p \tag{2.2a}$$

and

$$\langle q_n(x)q_{n'}(x')\rangle-\langle q_n(x)\rangle\langle q_{n'}(x')\rangle = p(1-p)\delta(n-n')\delta(x-x') . \tag{2.2b}$$

Here x labels the lattice site and n labels the time steps. The δ functions in (2.2b) are Kronecker δ functions of their (integer-valued) arguments,

$$S_n(x)=\begin{cases}1, & \text{if site } x \text{ is filled precisely at time } n,\\ 0, & \text{otherwise,}\end{cases} \tag{2.3}$$

and the $q_n(x)$'s are independent random variables taking on values 0 or 1. The product over y in (2.1) is a product over all nearest neighbors of the site x. The brackets $\langle\ \rangle$ denote an average over an ensemble of many clusters, so that Eqs. (2.2) just express the fact that the $q_n(x)$'s have an average value of p and are independent with respect to both x and n.

This model has a rich morphological structure and exhibits, in addition, very interesting and complex growth oscillation effects. The reader is referred to paper I and to Ref. 4 for a detailed description of these properties. A general familiarity with the results of paper I will be assumed in the rest of this paper.

The expression (2.1) is difficult to analyze both numerically and analytically. Numerically the difficulty arises because the stochastic noise, which increases as p decreases, necessitates averaging over many samples of clusters, or, alternatively, growing single clusters of a rather large size. Analytically, difficulties arise because of the complicated correlations between different $S_n(x)$'s resulting from the algorithm (2.1). It is, however, possible to simplify (2.1) so that analytical and numerical progress can be made more easily. To do this, we focus on a quantity of particular interest,

$$P_n(x)=\langle S_n(x)\rangle \tag{2.4}$$

and take an ensemble average of (2.1) approximating the right-hand side as a product of independent averages, viz.,

$$P_{n+1}(x)=\langle S_{n+1}(x)\rangle=\left\langle q_n(x)\left[1-\prod_y [1-S_n(y)]\right]\prod_{m=1}^{n}[1-S_m(x)]\right\rangle$$

$$\to\langle q_n(x)\rangle\left[1-\prod_y [1-\langle S_n(y)\rangle]\right]\prod_{m=1}^{n}[1-\langle S_m(x)\rangle] \tag{2.5}$$

so that

$$P_{n+1}(x)=p\left[1-\prod_{y}[1-P_n(y)]\right]\prod_{m=1}^{n}[1-P_m(x)]\ . \tag{2.6}$$

Equation (2.6) can be considered to be a kind of mean-field approximation to the stochastic equation (2.1), and defines the model that will be the object of study of most of this paper. Equation (2.6) is a rather complex deterministic iterative map for the quantities $P_n(x)$. As we shall see, it has morphological characteristics and exhibits growth oscillations which are qualitatively similar to those of (2.1). As such, enough of the important dynamics has been retained in (2.6) to provide a good first-order approximation to (2.1), as well as providing us with a system which is interesting in its own right. Moreover, as we shall discuss in Sec. V, it is possible to systematically generate a sequence of better approximations to (2.1), the first one of which is just (2.6).

We begin our study of the deterministic growth model (2.6) by demonstrating that the morphology of clusters grown according to this algorithm is qualitatively similar to those grown according to (2.1). To do this, we have solved (2.6) on a computer for various values of p on a two-dimensional square lattice with initial conditions

$$P_0(x)=\delta(x) \tag{2.7}$$

which just represents the existence of a single seed particle at the origin of the lattice. In Fig. 1 we show the overall cluster shapes obtained by using (2.6) up to 200 generations. To define the cluster shapes, we first note that the density $\rho(x)$ has the property

$$\rho(x)\propto\sum_{n}P_n(x)\ . \tag{2.8}$$

As we shall see in Sec. III, $\rho(x)$ has a complicated oscillatory structure, but beneath the oscillations and aside from some initial transients there is also an average uniform (but p-dependent) piece for $p>p_c=0.25$. The boundary of the clusters were defined by those points at which the density first fell to $\frac{1}{2}$ of its average value within the cluster. Except for values of p extremely close to p_c, this definition yields a clear and unambiguous definition of the cluster boundary. A comparison of Fig. 1 with Fig. 1 in Ref. 4 shows clearly that the general morphological characteristics of Eq. (2.1) and (2.6) are very similar indeed. Like (2.1), the deterministic model generates clusters which have a faceting transition (in this case, $p_f=0.5$) as well as a transition to "marginal growth" (in this case $p_c=0.25$).

The equation (2.6) [as well as its stochastic counterpart (2.1)] can be applied to a variety of situations in different dimensions and with different initial conditions. It is a simple exercise to write down the particular form of (2.6) which is applicable in different cases. Here we wish to display some of the forms which will be of particular interest for us in the rest of this paper. The situations we shall describe lead to equations that are one-dimensional, although the equation may describe an aspect of a growth process which takes place in more than one dimension.

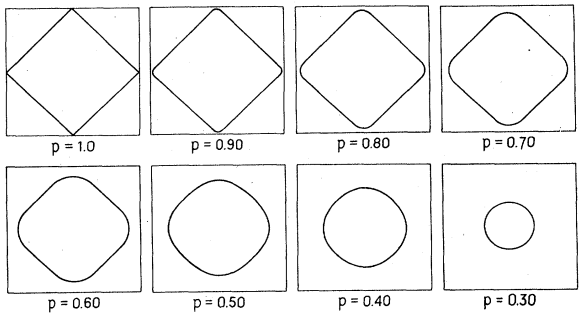

FIG. 1. Shape of clusters grown according to the deterministic model of Eq. (2.6) for various values of p.

The equations so generated all have a similar structure, but their differences nevertheless lead to interesting differences in their behavior, as we shall discuss below. For simplicity we limit ourselves to hypercubic lattices.

Consider first true one-dimensional growth along a line with initial conditions corresponding to a single seed particle at the origin. In this case (2.6) becomes

$$f_{n+1}(x)=1-p[1-f_n(x-1)f_n(x+1)]\prod_{m=1}^{n}f_m(x)\ , \tag{2.9}$$

where

$$f_n(x)=1-P_n(x)\ . \tag{2.10}$$

A close cousin of the process (2.9) is the case of two-dimensional growth with initial conditions which consist of an infinite line of seed particles along the y axis. In this case, because of the translational invariance in y, the growth is clearly a function only of the coordinate along the x axis, and (2.6) becomes

$$f_{n+1}(x)=1-p[1-f_n(x-1)f_n^2(x)f_n(x+1)]\prod_{m=1}^{n}f_m(x)\ , \tag{2.11}$$

which is similar, but not identical to (2.9).

Another important aspect of growth in two-dimensions is growth along a direction intersecting a facet. The simplest case to consider is growth along a ray oriented at 45° to a lattice axis. If we take as our initial conditions either (i) an infinite line of seed particles perpendicular to the direction of growth, or (ii) a single seed particle at the origin and wait long enough so that a clear facet of at least several lattice spacings has developed, then the growth along 45° will be essentially translationally invariant along the facet. In this case (2.6) becomes

$$f_{n+1}(x)=1-p[1-f_n^2(x-1)f_n^2(x+1)]\prod_{m=1}^{n}f_m(x)\ . \tag{2.12}$$

In (2.12) x labels the direction perpendicular to the facet. (Essentially, x labels rows of staggered lattice sites.)

It is easy to generalize (2.12) to higher dimensions. In d dimensions, for large enough p a cluster will have facets of dimension $1,2,\ldots,d-1$. For example, in three dimensions there will be, for large enough p, flat two-dimensional facets [oriented along the $(\pm1,\pm1,\pm1)$ directions] as well as sharp one-dimensional edges which lie in the planes defined by pairs of lattice axes. If we consider growth along a direction perpendicular to a $(d-1)$-dimensional facet, then, for values of p such that that facet exists, (2.6) becomes

$$f_{n+1}(x)=1-p[1-f_n^d(x-1)f_n^d(x+1)]\prod_{m=1}^{n} f_m(x)\ , \tag{2.13}$$

where (2.13) is understood to be applicable well within the facet region, i.e., for values of x and n for which the system is essentially translationally invariant perpendicular to the direction of growth. [Of course, if we wish to be more precise, we may say that (2.13) applies to growth from initial conditions which consist of an entire hyperplane of seed particles of dimension $d-1$, the normal to the hyperplane being in the direction $\hat{\mathbf{x}}_1+\hat{\mathbf{x}}_2+\cdots+\hat{\mathbf{x}}_d$.] We stress that (2.13) applies only in the region of a $(d-1)$-dimensional facet in d dimensions. In particular, the equations describing growth near a $(d-j)$-dimensional facet $(j>1)$ in d dimensions are not one dimensional.

III. DETERMINISTIC GROWTH IN ONE DIMENSION

In this section we will present a variety of numerical and analytical results for the simple case of purely one-dimensional deterministic growth governed by Eq. (2.9). In Sec. III A we will describe the general structure of this growth as a function of p and will discuss the features of (2.9) that are important in order to have oscillations. We will also display the results of numerical solutions for the density for some values of p. In Sec. III B we will show how to solve Eq. (2.9) to obtain analytic expressions for $P_n(x)$. In Sec. III C we will describe the structure of the cluster for p near p_c, and will show that the density falls off like a power of x when $p=p_c$.

A. General structure

The qualitative behavior of Eq. (2.9) is similar in many ways to the behavior observed for the stochastic model studied in paper I. In Fig. 2, for example, we have plotted the function $P_n(x)$ generated by Eq. (2.9) with the initial conditions (2.7) for $p=0.8$. In this figure the points represent the trail of all values of $P_n(x)$ for all n and x. The solid lines pass through $P_n(x)$ for selected values of n so that each curve represents the growing interface at a given time.[6]

This figure should be compared to Fig. 2(b) in paper I in which the same quantity along a lattice axis, defined by ensemble averaging, is plotted for the stochastic two-dimensional growth model discussed there. While they differ in detail, the two figures are clearly qualitatively similar. Moreover, if we plot $P_n(x)$ for different values of p, we see the same general trends for both the $d=2$ stochastic model along a lattice axis and the $d=1$ deterministic model, namely, the fundamental period of oscillation, which is determined, roughly, by the distance between the peaks of the broad curves in Fig. 2 [or Fig. 2(b) of paper I] decreases with decreasing p. This behavior will be explained in more detail in Sec. IV. In addition, the amplitude of the oscillations tends to increase with decreasing p. Furthermore, in both models there is a critical value of p, p_c, at which growth becomes marginal. Thus, both models share the same scenario: For $1>p>p_c$, the algorithm grows a structure with finite overall background density and with oscillations on top of that. As $p\to1$ the oscillations become longer in period and smaller in amplitude, and the growth becomes relatively more uniform.[7] As $p\to p_c$, the fundamental period goes to zero. This we understand, in a sense that will become clearer below, as a limit cycle becoming a fixed point. Moreover, when $p=p_c$ the fixed point is the trivial fixed point since, when $p=p_c$, $P_n(x)\to0$ for large x and n. As we shall see in Sec. III C, at $p=p_c$ the growth is marginal with a power-law-behaved density analogous to fractal behavior.

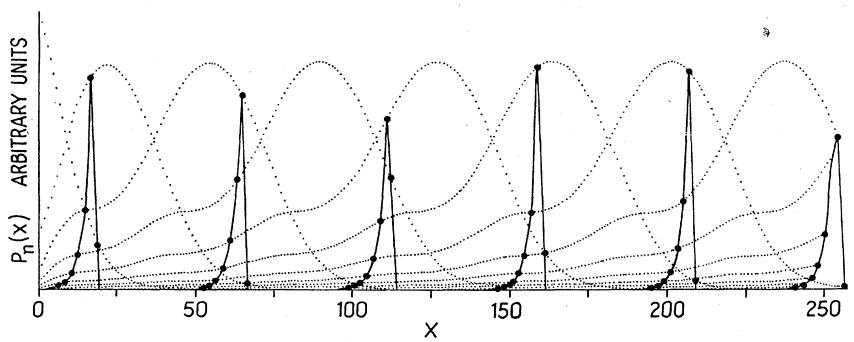

FIG. 2. $P_n(x)$ as a function of x along a lattice axis for the deterministic model (2.6) in two dimensions with $p=0.8$. The heavy dots, connected for visual clarity by solid lines, represent the values of $P_n(x)$ for a fixed n. Values for $n=20$, 70, 120, 170, 220, and 270 are shown.

Thus, kinetic fractal growth is controlled by the trivial fixed point of the appropriate functional stochastic or deterministic map analogous to (2.9).

By studying (2.9) further, we can derive a number of other results which will be helpful in elucidating the general characteristics of such maps. First, it is simple to derive the value of p_c for (2.9). To do that, we recall as $p \to p_c$, $P_n(x)$ is small for large n and x, and so we can linearize (2.9) in $P_n(x)$. We can then sum over n on both sides of the equation to obtain an expression for the density $D(x) \equiv \sum_n P_n(x)$. To deduce a value for p_c, it is sufficient to keep only linear terms in $D(x)$. In this approximation we have

$$D(x) = p[D(x+1) + D(x-1)] , \tag{3.1a}$$

$$\partial_x^2 D(x) \cong (1-2p) D(x) + \cdots . \tag{3.1b}$$

For $p < p_c = \frac{1}{2}$ the physically acceptable solution of (3.1b) is exponentially falling with x. For $p > p_c$ $D(x)$ has oscillatory behavior as a function of x. For $p = p_c = \frac{1}{2}$, the linear term on the right-hand side vanishes and the behavior is determined by nonlinear terms. In Sec. III C the behavior of (2.9) at $p = p_c$ will be discussed more carefully, and the power-law behavior of the density of the cluster at $p = p_c = \frac{1}{2}$ will be derived.

It is interesting to compare this value of p_c with the value obtained for the closely related problem defined by (2.11). Linearizing that equation and applying the same reasoning that led to (3.1) we find $p_c = \frac{1}{4}$. That these values of p_c are correct is intuitively obvious when we recall that in model (2.9) each growth site has two nearest neighbors and in (2.11) each growth site has four nearest neighbors.

Another lesson to be learned from studying (2.9) is the conditions necessary to obtain oscillatory behavior. In particular, consider (2.9) without the last factor, i.e.,

$$f_{n+1}(x) = 1 - p[1 - f_n(x-1) f_n(x+1)] . \tag{3.2}$$

It is not difficult to see that with the initial conditions (2.7) this iterative map does not have the oscillating structure of (2.9). In Fig. 3, for example, we have plotted $P_n(x)$ generated by (3.2) for $p = 0.8$. The reason there is no oscillatory structure is just that there are no competing terms in the iterative map. In order to have oscillations we need such competitive interactions. The simplest example of this is competition between the linear and quadratic terms in the Feigenbaum map.[8] The last factor in (2.9) provides the necessary competition. Physically what happens is this: A site has a better chance of being occupied at time n the more likely it is that its neighbors are occupied at time $n-1$. On the other hand, the more likely its neighbors are to be occupied at time $n-1$, the more likely the site in question is to be occupied at time $n-1$. [Roughly speaking, this is the information contained in the last factor of (2.9).] The competition between these two effects is necessary for growth oscillations. Furthermore, this same competition gives rise to a moderately well-defined interface for the growing structure, which, as we have argued elsewhere[1,2] is a necessary ingredient for understanding the existence of growth oscillations from a different point of view. To see this clearly, look again at Fig. 3. Notice that $P_n(x)$ for fixed n as a function of x is very broad (extending all the way to $x = 0$) compared with the similar quantity plotted in Fig. 2. There are no limiting terms to suppress the small x tail of $P_n(x)$ for fixed n in Fig. 3, so that the growing interface does not stay narrow. Note finally that while the last factor in (2.9) is physically motivated for our growth process, a much simpler form would also give rise to growth oscillations. To get oscillatory structure in this simple example, we need only keep a finite number of factors, $f_m(x)$, near $m = n$.

To complete our survey of the general structure of equations such as (2.9), it is interesting to plot the density of a growing one-dimensional cluster as a function of x for various values of p. The density oscillations generated by (2.9) are small enough in amplitude to be rather sensitive to numerical rounding errors in computer calculations. However, the oscillations of the related equation (2.11) are somewhat more pronounced and are unaffected by numerical errors in the computation. In Fig. 4, therefore, we have plotted the density as a function of x for the

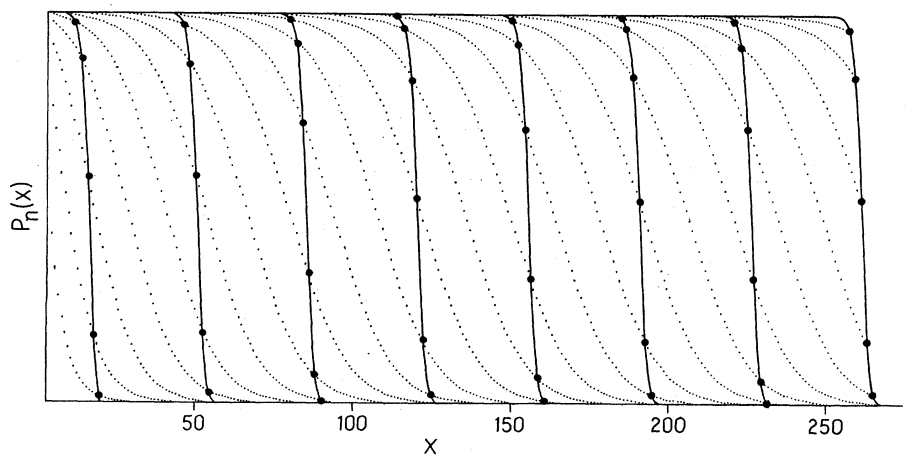

FIG. 3. $P_n(x)$ as a function of x for the model defined by (3.2). This figure was generated by iterating (3.2) for 300 generations. The heavy dots, connected for visual clarity by solid lines, represent the values of $P_n(x)$ for fixed n. Values for $n = 20$, 60, 100, 140, 180, 220, 260, and 300 are shown.

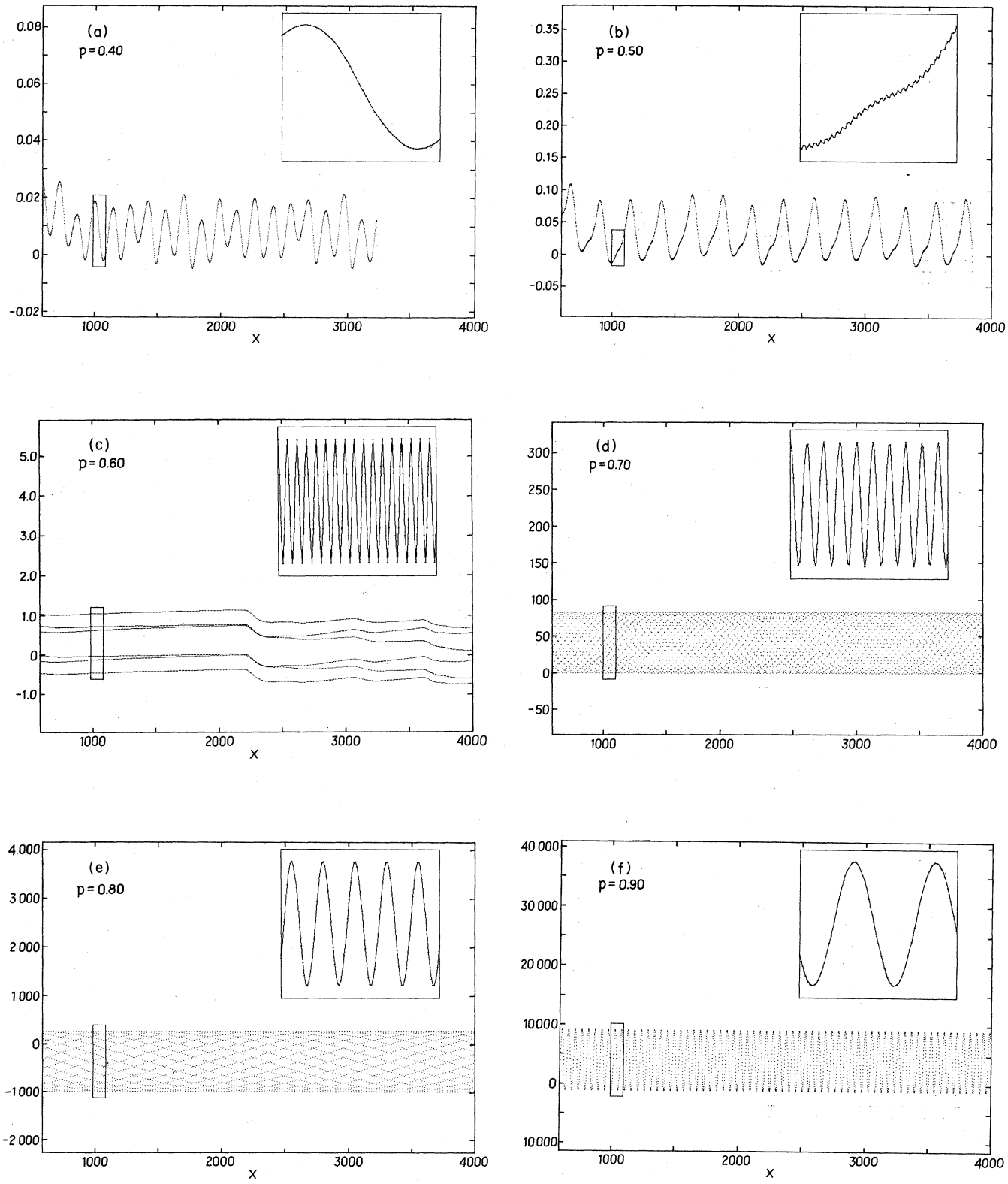

FIG. 4. Density as a function of x for one-dimensional deterministic growth governed by Eq. (2.11) for various values of p. For each curve a detail is shown in the upper right-hand corner. For all graphs $\bar{\rho}(x)$ was determined by averaging over the region $600 \leq x \leq 4000$ to eliminate initial transients. The vertical axis is $[\rho(x)-\bar{\rho}]\times 10^6$. (a) $p=0.4$, (b) $p=0.5$, (c) $p=0.6$, (d) $p=0.7$, (e) $p=0.8$, (f) $p=0.9$, (g) $p=0.5290$, (h) $p=0.5291$.

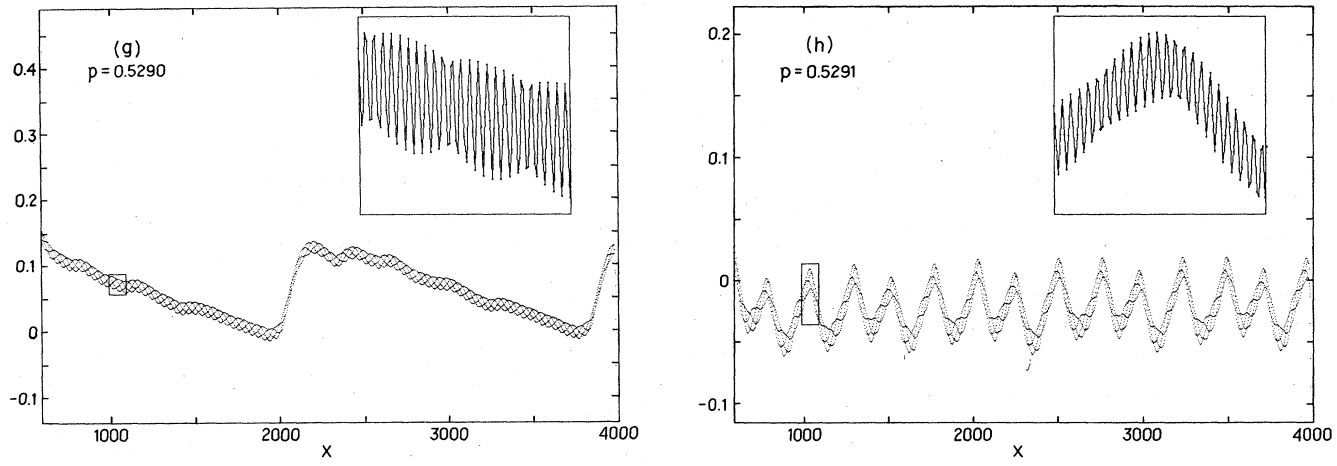

FIG. 4. (*Continued*).

equation (2.11). Most qualitative observations we wish to make apply to (2.9) as well. (Note, however, that the critical values of p are different in the two cases.) From these figures we can deduce two important characteristics of the density of this model. First, the density clearly has a complex, multiperiodic structure. In fact, in general, we should expect contributions from Fourier components with wavelengths up to the order of the size of the cluster. This can be understood by referring to Fig. 2 [which, although it was generated by (2.6), is qualitatively similar to the analogous curves generated by (2.9) and (2.11)] in which we see that the broad dotted curves are not identical one to the next, but have increasingly long tails dying off toward the origin. Since $\rho(x)\sim\sum_n P_n(x)$, these long tails will modulate the density on a period of the order of the size of the cluster. This multiperiodicity is also consistent with what was observed in paper I for the stochastic model.

In Sec. IV, when we discuss analogous oscillations in a related quasi-one-dimensional model, we will present a qualitative explanation of the oscillations that should help to clarify the nature of the multiperiodic structure as well as the dependence of the fundamental period on ρ. Second, the oscillatory structure of $\rho(x)$ can be incredibly sensitive to small changes in p, as we see by comparing Figs. 4(g) and 4(h). In these figures p differs by 10^{-4}.

B. Analytic solution of one-dimensional deterministic growth

In this section we will show how to solve Eq. (2.9) analytically. Our method of solution will provide us with a hierarchy of linear equations for functions describing the dotted line curves such as those shown in Fig. 2. With minor modifications the technique can be applied to any quasi-one-dimensional growth process such as that expressed in Eq. (2.11).

To begin, we first change variables in (2.9) and consider f as a function of $L\equiv x-n$ and n, rather than as a function of x and n. Define

$$r_n(L)=f_n(x)\ , \tag{3.3}$$

then (2.9) becomes

$$r_{n+1}(L-1)=1-p[1-r_n(L+1)r_n(L-1)]\times\prod_{i=0}^{n}r_i(L+n-i)\ . \tag{3.4}$$

[Note: The argument of the function r is the value of x to which the corresponding f in (3.3) refers, minus the subscript of the r. So, for example, if in (3.4) we pick a value of n and x, say (n_0,x_0) such that $L=L_0=x_0-n_0$, then the argument of r_i in the last factor of (3.4) is just L_0+n_0-i, which corresponds to a value of $x=(L_0+n_0-i)+i=L_0+n_0=x_0$, as it should.]

Now, since the moving interface can never propagate faster than one lattice spacing per time step, and since our initial conditions consist of a single seed particle at the origin, it is clear that $r_n(L)=1$ for any $L>0$, and for any n. Using this we can simplify (3.4). If we set, in (3.4), $L=1$ then we have

$$r_{n+1}(0)=1-p[1-r_n(0)]\ , \tag{3.5a}$$

$$r_0(0)=0\ , \tag{3.5b}$$

where (3.5b) just expresses the initial condition of a seed particle at the origin. Equation (3.5) is an easily solved linear equation for the function $r_n(0)$ as a function of n. This information can now be used to determine the $r_n(A)$ for other values of A by using (3.4) with other value of L. If we set $L=0$ in (3.4) we have

$$r_{n+1}(-1)=1-p[1-r_n(-1)]r_n(0)\ , \tag{3.6a}$$

$$r_0(-1)=r_0(-2)=\cdots=1\ . \tag{3.6b}$$

Equation (3.6a) is a linear equation for $r_n(-1)$ which, with the initial conditions in (3.6b) and the function $r_n(0)$, can be solved. It is easy to see that the only physically acceptable solution for $r_n(-1)$ is $r_n(-1)=1$. This is because the growth algorithm forbids the occupancy of odd (even) sites at even (odd) times. Next, setting $L=-1$ in (3.4) yields

$$r_n(-2)=1-p[1-r_n(-2)r_n(0)]r_n(-1)r_n(0)\ , \tag{3.7}$$

which, given (3.6b), $r_n(0)$, and $r_n(-1)$, can be solved for $r_n(-2)$. In general we can set $L=-2l$, and define

$t_n(-l)=r_n(L)$ [to eliminate the trivial functions $r_n(L)$ for odd L] in (3.4), and we have

$$t_{n+1}(-l)=1-p[1-t_n(-l)t_n(-l+1)] \times t_{n-1}(-l+1)t_{n-3}(-l+2)\cdots t_{n-2l+1}(0)\ , \tag{3.8}$$

so that the function $t_n(-l)$ can be solved in terms of the functions $t_n(-A)$ with $0\le A<l$.

We can easily write down the general solution of (3.8). We note that it has the form

$$t_{n+1}(-l)=h_n(-l)+g_n(-l)t_n(-l)\ , \tag{3.9}$$

where the coefficients are given by

$$h_n(-l)=1-pt_{n-1}(-l+1)t_{n-3}(-l+2)\cdots t_{n-2l+1}(0) \tag{3.10}$$

and

$$g_n(-l)=[1-h_n(-l)]t_n(-l+1)\ .$$

The general solution of (3.9) is

$$t_{n+1}(-l)=t_0(-l)\prod_{i=0}^{n} g_i(-l) + \left[\sum_{j=0}^{n}\frac{h_j(-l)}{\prod_{i=0}^{j} g_i(-l)}\right]\prod_{i=0}^{n} g_i(-l)\ . \tag{3.11}$$

Clearly, the complete set of functions $r_n(L)$ is equivalent to the complete set of function $f_n(x)$. But what are these $r_n(l)$'s? These just describe the dotted-line curves that appear in figures such as Fig. 2. The curves are labeled by $-l$, so that $1-t_n(-l)$ considered as a function of n for fixed l just describes one of the broad dotted curves in the figure. To see that this is so, consider two successive points on one of the dotted curves. Let the first point represent some value of $P_n(x)$, i.e., the probability that the site x is occupied at time n. The next point to the right along the same curve just represents the probability that site $x+1$ is occupied at time $n+1$ which is $P_{n+1}(x+1)$. But $t_n(-l)=t_n(x-n)=f_n(x)=1-P_n(x)$, and $1-P_{n+1}(x+1)=f_{n+1}(x+1)=t_{n+1}[x+1-(n+1)]=t_{n+1}(x-n)=t_{n+1}(-l)$ so that both points share the same value of l. Thus, $1-t_n(-l)$ as a function of n describes the broad dotted curves as a function of x. The first dotted curve corresponds to $l=0$, the next to $l=1$, and so forth.

The expressions for these curves are simple for low values of $|l|$ and get progressively more complicated as $|l|$ increases. For example,

$$t_n(0)=1-p^n\ , \tag{3.12}$$

$$t_n(-1)=p^n\left[\prod_{i=0}^{n-1}(1-p^i)\right] \times\left[1+\sum_{j=0}^{n-1}\frac{1-p+p^{j+1}}{p^{j+1}\prod_{k=0}^{j}(1-p^k)}\right]\ . \tag{3.13}$$

We have plotted these functions directly and have checked that they reproduce the curves generated by direct use of Eq. (2.9).

This procedure for solving (2.9) can be thought of as a method of approximating the structure of the growing cluster by retaining contributions of successively longer wavelength. This can be most easily understood in terms of the density, which, as we saw has a complicated multiperiodic structure. Suppose we solve for $t_n(0)$, $t_n(-1)$, $t_n(-2)$, $t_n(-3)$, and $t_n(-4)$ and plot them as in Fig. 5(a). It is clear that a good approximation to the structure of the cluster as given, say, by its density would be to take the segment of Fig. 5(a) that lies between the intersection of the $l=1$ and $l=2$ curve [point A in Fig. 5(a)] and the intersection of the $l=2$ and $l=3$ curve (point B) and simply repeat it as shown in Fig. 5(b). (We have chosen to repeat this segment rather than the one lying between point O and A since the region OA still includes significant transient effects.) This will capture much of the oscillatory structure of the density, and, in particular, will include the strong effects of the fundamental period. If we solve, in addition for $t_n(-5)$, then we can get a better approximation by plotting all six curves and taking the segment that lies between the intersection of the $l=1$ and $l=2$ curves and the intersection of the $l=3$ and $l=4$ curves [point C in Fig. 5(a)] and repeating that. This will include not just the effect of the fundamental period, but also the effect of some modulations of it on a longer length scale. Since the oscillations with shorter periods seem to have, in general, the largest amplitude, a fairly low order of this approximation should give a reasonable description of the growing structure. From Fig. 2 it is clear that one major contribution to the very long-wavelength oscillations is the long low tail of the curves with larger values of $|l|$ which contribute only a small amplitude modulation to the density. Notice also how closely the lower contributions from the $l=3$ and $l=4$ curves match when we repeat the segment AB.

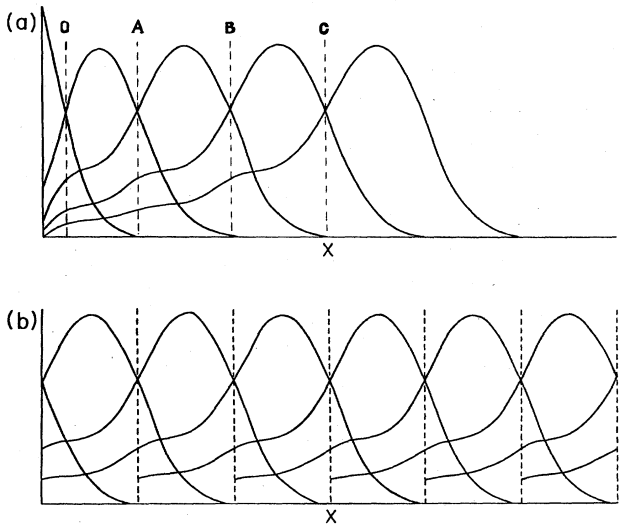

FIG. 5. (a) The function $t(0)$, $t(-1)$, $t(-2)$, $t(-3)$, and $t(-4)$ from Fig. 2. (b) Repetition of the segment AB in (a).

C. Behavior for p near p_c

In Eq. (3.1) we derived p_c, the value of p below which the cluster grows only to a finite size. We found $p_c=\frac{1}{2}$. Here we wish to study the behavior near p_c in a little more detail. In particular, we want to calculate the "fractal dimension" (i.e., the power of x with which the density falls off) of the cluster defined by (2.9) at p_c, and we want to understand, qualitatively what happens to the curves of constant $x-n$ derived in Sec. II as $p\to p_c^+$.

To begin, we note that for p near p_c, $P_n(x)$ will get small as n and x get large. Since we are interested in the asymptotic behavior of the cluster in this region, we can expand (2.9) in powers of $P_n(x)$. Doing so, and keeping terms of order $P_n^2(x)$, we have

$$P_{n+1}(x)=p\left[P_n(x-1)+P_n(x+1)-P_n(x-1)P_n(x+1)-[P_n(x+1)+P_n(x-1)]\sum_{m=0}^{n}P_m(x)\right]. \tag{3.14}$$

In Eq. (3.14), let us now take x large and fixed and sum over n. Defining

$$D(x)=\sum_{m=0}^{\infty}P_m(x)\,, \tag{3.15}$$

we have

$$D(x+1)+D(x-1)-\frac{1}{p}D(x)=\sum_{n=0}^{\infty}P_n(x+1)P_n(x-1)+\sum_{n=0}^{\infty}\left[[P_n(x+1)+P_n(x-1)]\sum_{m=0}^{n}P_m(x)\right]. \tag{3.16}$$

$D(x)$ is clearly just the density of the cluster as a function of x.

Now let us try to simplify the terms on the right-hand side of (3.16). Our object is to obtain an equation for $D(x)$ which is accurate in form for large x so that we can deduce the asymptotic behavior of $D(x)$. We are not concerned with computing precise values of coefficients here, but only with discovering which are the leading nonzero terms in the asymptotic limit. First, we note that in the last term on the right-hand side of (3.16) we can replace

$$\sum_{m=0}^{n}P_m(x)\to\sum_{m=0}^{\infty}P_m(x)=D(x)\,. \tag{3.17}$$

To justify this, note that for x fixed $P_n(x)$ will be essentially zero for n sufficiently small and sufficiently large. If n is sufficiently large for fixed x then clearly $\sum_{m=0}^{n}P_m(x)\cong D(x)$. If n is small enough so that the primary contribution to $D(x)$ is missing from $\sum_{m=0}^{n}P_m(x)$, we can still make the replacement (3.17) in (3.16), since for these values of n the coefficient of $\sum_{m=0}^{n}P_m(x)$ will be essentially zero anyway. [Note that we assume that $P_n(x)$ is a moderately smooth function of x for large enough x.] Thus, to leading order, the last term on the right-hand side of (3.16) becomes

$$\sum_n[P_n(x+1)+P_n(x-1)]\sum_{m=0}^{n}P_m(x)\to[D(x+1)+D(x-1)]D(x)\,. \tag{3.18}$$

The first term on the right-hand side may, for our purposes, be replaced by an upper-bound. It is certainly true that

$$0<\sum_n^{\infty}P_n(x+1)P_n(x-1)\le D(x+1)D(x-1)\,. \tag{3.19}$$

As we shall see, when $p=p_c$ the leading behavior of $D(x)$ for large x will come from terms on the right-hand side of (3.16) proportional to $D^2(x)$. Since both terms on the right-hand side of (3.16) have the same sign, the first term can, at most, alter the value of the coefficient of the $D^2(x)$ which will not affect our results for the behavior of the density with x. To demonstrate this, we will replace in (3.16)

$$\sum_n^{\infty}P_n(x+1)P_n(x-1)\to\alpha D(x+1)D(x-1) \tag{3.20}$$

and show that the form of the asymptotic behavior (i.e., the exponent of x) is insensitive to the value of α.

Using (3.20) and (3.18) in (3.16), and further expanding

$$D(x+1)=D(x)+D'(x)+\tfrac{1}{2}D''(x) \tag{3.21}$$

we have

$$D''(x)+\left[2-\frac{1}{P}\right]D(x)\cong(2+\alpha)D^2(x)-\alpha[D'(x)]^2+(1+\alpha)D(x)D''(x)\,, \tag{3.22}$$

where we have kept terms up to second order in derivatives with respect to x.

What does (3.22) imply for the large x behavior of $D(x)$ for various values of p? When $p\neq p_c$ there is a term proportional to $D(x)$, and so we may ignore all the terms on the right-hand side of (3.22). We find then that

$$D(x)\sim\exp[-i(2-1/p)^{1/2}x],\quad p\neq p_c\,. \tag{3.23}$$

For $p>p_c\equiv\frac{1}{2}$ $D(x)$ given by (3.23) is oscillatory. This solution for $p>p_c$ is not necessarily consistent with the assumptions used to obtain (3.22). Nevertheless it is indicative of the fact that $D(x)\not\to 0$ for large x when $p>p_c$. For $p<p_c$, (3.23) shows us that $D(x)$ falls exponentially with x. That is to say, the cluster grows only to a finite size, even in the $n\to\infty$ limit, as we expect for $p<p_c$. When $p=p_c=\frac{1}{2}$, the coefficient of the $D(x)$ term is zero, and we must keep the terms on the right-hand side of (3.22). For large x, the leading behavior is determined by the first term on the right-hand side of (3.22) and we find

$$D(x)\sim x^{-2}+\cdots,\quad p=p_c\,. \tag{3.24}$$

The other terms, involving derivatives on the right-hand

side of (3.22) will control higher-order corrections to the asymptotic behavior given in (3.24). Note that the exponent in (3.24) is independent of α ($\alpha > 0$), as promised above. Because the arguments leading to (3.22) are a bit loose, we have also solved (2.9) numerically, on a computer for $p = p_c = \frac{1}{2}$. We found that the asymptotic behavior of $D(x)$ is that predicted by (3.24). Thus, the one-dimensional deterministic model (2.9) has a power-law-behaved density for $p = p_c = \frac{1}{2}$. This expression of marginal growth is the closest our simple one-dimensional model can come to mimicking fractal behavior. True fractal growth will occur in the more realistic higher-dimensional stochastic models described elsewhere.

IV. DETERMINISTIC GROWTH OF FACETS

In addition to the equation studied in Sec. III, it is useful to study Eq. (2.13) which is a quasi-one-dimensional equation describing growth normal to a $(d-1)$-dimensional facet in d dimensions, as described in Sec. II. We will find that as a function of p, the growth described by this equation has two "critical points." The first, p_f, is the value of p below which there are no facets (in a sense to be described below). The second, p_c, is the value of p below which the probability to continue growing to infinity is zero. Our purpose in this section is not to determine all the details of the behavior of (2.13). Rather, we shall apply the methods of solution of Sec. III to determine the general behavior of the growth governed by (2.13). In so doing we will gain additional insight into the origin and nature of the growth oscillations.

Before beginning, it is useful to stress a point made in Sec. II. Equation (2.13), properly speaking, describes growth along the direction $\underset{\sim}{z} = \sum_{i=1}^{d} \hat{\mathbf{x}}_i$, where $\hat{\mathbf{x}}_i$ is a unit vector in the i direction on a d-dimensional hypercubic lattice, and where the initial conditions are a $(d-1)$-dimensional surface of seed particles normal to $\underset{\sim}{z}$. Concerning growth from a single seed particle in d-dimensions, this equation is relevant to the local description of the growth perpendicular to a $(d-1)$-dimensional facet when such a facet exists. Equation (2.13) assumes translational invariance in directions perpendicular to $\underset{\sim}{z}$. When there is no facet in growth from a single seed such translational invariance disappears and (2.13) is no longer relevant to the description of that situation. Nevertheless, Eq. (2.13) with $p > p_f$ does, qualitatively at least, describe growth normal to the facet when such a facet exists. Moreover, the value of p_f determined from (2.13) is, at least in the deterministic model discussed here, the same as the value of p at which the corresponding facet disappears in growth from a single seed particle. We expect this identity to survive also in the corresponding stochastic models.

In the stochastic model studied in paper I, it was observed that for directions normal to a facet there were apparently no strong growth oscillations. An analogous situation obtains for Eq. (2.13). To see how this comes about, let us apply the method of Sec. III to solve Eq. (2.13). As before, we define $L = x - n$, and

$$r_n(L) = f_n(x) \tag{4.1}$$

so that (2.13) becomes

$$r_{n+1}(L-1) = 1 - p[1 - r_n^d(L+1) r_n^d(L-1)] \times \prod_{i=0}^{n} r_i(L+n-i) \, . \tag{4.2}$$

Setting $L = 1$ in (4.2) yields

$$r_{n+1}(0) = 1 - p[1 - r_n^d(0)] \, . \tag{4.3}$$

For any d and $p \leq 1$ (4.3) has a (trivial) fixed point at $r(0) = 1$. For $d = 1$ and $p < 1$ this is the only fixed point. It is attractive and corresponds, as we saw in Sec. III, to the situation in which $P_n(x = n) \to 0$. This is just a statement of the fact that the average growth velocity of the cluster is less than one lattice per time step. [In fact, as we saw in Sec. III, all $r_n(L) \to 0$ as $n \to \infty$ for this case so that all $P_n(x = n + L) \to 0$ for all finite $L \leq 0$. This means that the velocity of growth is *strictly* less than one lattice spacing per time step. It is, on average, a finite fraction of a lattice spacing per time step.] For $p = 1$ there is another fixed point of (4.3) which is $r(0) = 0$, and corresponds to dense, regular, uniform, and boring growth.

For $d > 1$ the situation is somewhat different. For $1/d < p < 1$ there is a nontrivial fixed point of (4.3) which is attractive and for which $0 < \lim_{n \to \infty} r_n < 1$. For example, for $d = 2$, $\lim_{n \to \infty} r_n(0) = (1-p)/p$. This tells us that for $1/d < p < 1$ there is a finite probability for the cluster to grow n lattice spacings in n time steps so that the growth velocity is one lattice spacing per time step. In growth from a single seed particle, this is the situation that gives rise to a facet. Thus the faceting transition p_f associated with (2.13) is $p_f = 1/d$. Let us first analyze the behavior of the growth implied by (2.13) for $1 \geq p > p_f$. The case $p < p_f$ will be discussed below.

Let us study the asymptotic behavior of the $r_n(L)$ for $|L| > 0$. Setting, for example, $L = 0$ in (4.2), we have

$$r_{n+1}(-1) = 1 - p[1 - r_n^d(-1)] r_n(0) \, . \tag{4.4}$$

We can use the solution of (4.3) in (4.4) to solve for $r_{n+1}(-1)$. To find the fixed-point behavior of $r(-1)$, though, it is sufficient to take $n \to \infty$ on both sides of (4.4) and insert the fixed-point value of $r(0)$. Thus,

$$r(-1) = 1 - p[1 - r^d(-1)] r(0) \, , \tag{4.5}$$

where

$$r(L) \equiv \lim_{n \to \infty} r_n(L) \, .$$

Equation (4.5) has the same form as (4.3) with $n \to \infty$, except that $p \to pr(0)$. Thus, for example, for $d = 2$, two values of $r(-1)$ satisfy (4.5), namely 1 and $p/(1-p)$. For $\frac{1}{2} < p < 1$, only the solution $r(-1) = 1$ is physically acceptable. In fact $r_n(-1) = 1$ for all n, and here again we see the fact that our algorithm forbids occupancy of an even (odd) site at odd (even) time.

As in Sec. III, we proceed to sequentially solve for the $r_n(L)$ for larger values of $-L$. It is not difficult to see that the result is that the attractive fixed point[9] for $r_n(L)$ for even L is strictly between zero and one for $1/d < p < 1$ and goes to 1 both for $p = 1$ and $p = 1/d$. For example, it

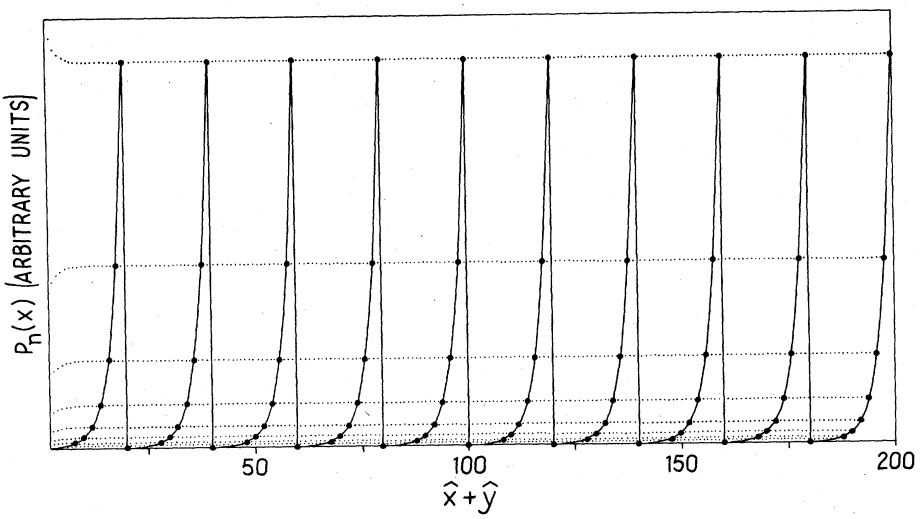

FIG. 6. $P_n(x)$ for Eq. (2.13) with $p=0.7$ and $d=2$. In terms of two-dimensional growth, this figure represents growth normal to a facet (at 45° to a lattice axis). Again, the heavy dots represent values of $P_n(x)$ for a fixed value of n, as a function of x, and are connected by solid lines for visual clarity. Curves for $n=40$, 80, 120, 160, 200, 240, 280, 370, 360, and 400 are shown. This figure was generated by iterating (2.13) for 400 generations.

is a straightforward matter to solve for $r(-2)$ for $d=2$, and we find that the nontrivial attractive fixed point is at

$$r(-2)=\frac{p^2-[p^4-4p^3(1-p)^3]^{1/2}}{2(1-p)^3} \tag{4.6}$$

which is between 0 and 1 for $\frac{1}{2}<p<1$ and is equal to 1 for $p=\frac{1}{2}$ and 1, as expected.

How do we interpret these results? Recall that the function $r_n(L)$ is just

$$r_n(L)=1-P_n(x=n+L) \tag{4.7}$$

so that $\lim_{n\to\infty}[1-r_n(L)]$ is just a measure of the probability for the cluster to occupy the $(n+L)$th lattice site at the time n. (Remember that $L\leq 0$.) If $r(L)=1$ for any (finite) L then the growth velocity is strictly less than 1. If $0<r(L)<1$, then the growing edge of the cluster will propagate with a velocity equal to 1 lattice spacing per time step.

In Fig. 6 we have plotted $P_n(x)$ determined by Eq. (2.13) with $d=2$ for $p=0.7$. Notice the following important features: (i) The curves for fixed L have a nonzero asymptotic value which is reached exponentially from the origin. (ii) The asymptotic values $r(L)$ must decrease rapidly enough with L to ensure that $\sum_n P_n(x)$ for fixed, large x converges, since this is just a measure of the net probability for the site x to be occupied. (iii) There is no evidence of any oscillatory structure. After the initial transients have died out (which for $p>p_f=\frac{1}{2}$ occurs exponentially fast) the cluster grows in a smooth nonoscillating way. This is consistent with our picture of the physical origin of growth oscillations: For $p>p_f$, the propagation of the cluster is locked to the underlying lattice. There is no possibility for beating, or incommen-

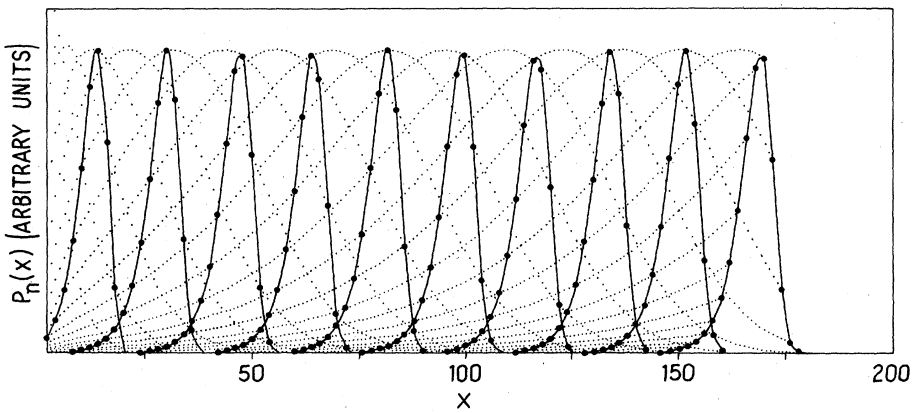

FIG. 7. $P_n(x)$ determined by Eq. (2.13) for $d=2$ and $p=0.4$. Here $p<p_f=0.5$ for this equation and we see clearly the existence of oscillations. There is no simple relation of this figure to bona fide two-dimensional growth. Heavy dots connected by solid lines again represent $P_n(x)$ for fixed n as a function of x. Curves for $n=40$, 80, 170, 160, 200, 240, 280, 320, and 400 are indicated. This figure was generated by iteration (2.13) for 400 generations.

surations to develop, and so there are no oscillations.

For $p < p_f$, the situation is entirely different. There $\lim_{n\to\infty} r_n(L) \to 1$, and the picture that develops is like that shown in Fig. 7 where we have plotted $P_n(x)$ determined by Eq. (2.13) with $d=2$ and $p=0.4$. Notice the qualitative similarity with Fig. 2.

A very simple, qualitative argument can be used to understand the general features of the curves shown in Fig. 7, or Fig. 2, or the analogous results in stochastic models. This argument will allow us to understand qualitatively the shapes of the L curves, the existence of maxima in these curves, and the positions of these maxima. The argument is based on the fact that in all these cases, the average growth velocity is a fraction of a lattice spacing per time step. Because the growth velocity λ for these processes is less than one lattice spacing per time step, $P_n(n+L) \to 0$ for large n and fixed L. On the other hand, since $\lambda < 1$, we may estimate λ by $(a-2)/a$ where a is an integer. The best such estimate will be obtained by $a=a^*$ such that $|(a^*-2)/a^*-\lambda|$ is a minimum. Thus, the lattice site that is most likely to be occupied at time a^* is roughly given by $x=a^*-2$, and so the curve with $L=x-n=a^*-2-a^*=-2$ will have a maximum near $x=a^*-2$. Similarly, if we find the best approximation to λ of the form $(b^*-4)/b^*$ with b^* an integer, then the curve with $L=-4$ will have a maximum near $x=b^*-4$. In general, b^* will be close to $2a^*$, although not necessarily exactly so. It is clear that the process continues and the extent to which the integers in higher-order estimates are not integer multiples of those in lower order estimates gives rise to some of the multiperiodic effects.

With this picture we can also understand the observation that the fundamental period of the oscillation increases as p increases [e.g., in Eq. (2.13) as $p \to p_f^-$]. As p increases λ increases also, and so the a^* which minimizes $|(a^*-2)/a^*-\lambda|$ will be larger. Thus, the peak in the $L=-2$ curve will occur at larger x, and the distance between a^* and b^* will likewise increase. But this distance is approximately the fundamental period of oscillation.

On the basis of this simple argument, we therefore conclude that, because $\lambda < 1$, (i) there are peaks in the L curves whose position can be easily estimated, (ii) the fundamental period of the growth oscillations is approximately the distance between peaks in these L curves, and (iii) this fundamental period increases as λ gets closer to one, which, generally means p increasing in a domain in which there are oscillations. Refinements of this argument can be used to help understand the multiperiodic nature of growth in more detail. This will be done elsewhere.

Thus, we have arrived at an understanding of the general behavior of (2.13) as a function of p. For $p > p_f = 1/d$ growth proceeds with an average velocity of one lattice spacing per time step. In this regime there are no growth oscillations. This corresponds to growth normal to a facet in growth from a single seed particle. For $p < p_f$ the average growth velocity λ is less than 1, and growth oscillations appear because of induced beating between the average distance traveled per time step and the lattice spacing. The fundamental period of oscillation decreases as p decreases from p_f.

Finally, there is another critical point associated with (2.13), p_c, below which the cluster does not grow indefinitely large. The analysis of (2.13) for p near p_c is similar to the analysis of (2.9) for p near p_c, as discussed in Sec. III C, and the behavior is quite analogous. For (2.13) it is easy to see that $p_c = 1/2d$. As $p \to p_c^+$, the fundamental period of the growth oscillations decreases, the peaks between curves of constant L merge, and the average growth velocity λ goes to zero as $p \to p_c$. At this point the growth is marginal and has a density which is, in general, power-law behaved as a function of x. For $p < p_c$ the cluster grows only to a finite size (the density falling exponentially with x), and has zero probability to grow indefinitely as a function of n.

V. RELATIONSHIP BETWEEN THE STOCHASTIC AND DETERMINISTIC MODELS

The deterministic models we have discussed, while interesting in their own right, are also approximations to the stochastic models of Refs. 1 and 2. In the sense discussed in Sec. II, they may be considered to be mean-field-like approximations to the stochastic models. In this section we wish to elucidate this connection by describing a sequence of approximations whereby the stochastic model may be approached starting with the deterministic model. For our purposes it will be sufficient to discuss this connection in the context of the one-dimensional realization of (2.1), whose deterministic counterpart is (2.9). Application of the method to other models in higher dimensions is, in principle, straightforward. Before beginning, let us recall that in one dimension (2.1) is trivial in the sense that for $p < 1$ growth is always damped exponentially so that the probability of growing a cluster to arbitrarily large size is strictly zero. On the other hand, when $p=1$, the one-dimensional cluster grows densely and uniformly forever. Thus, in this sense, $p_c = 1$ for (2.1) in one dimension. On the other hand, $p_c = \frac{1}{2}$ for (2.9), the deterministic version of (2.1). We will show how our sequence of approximations improves the estimate for p_c in this simple model.

The sequence of approximations we have in mind is rather obvious. The zeroth-order approximation, (2.9), results from taking independent averages over the $S_n(x)$ on both sides of (2.1). To obtain the first-order approximation, we simply iterate (2.1) once before taking averages. We have then

$$t_{n+2}(x) = 1 - q_{n+1}(x)\left[1 - [1 - q_n(x+1)[1 - t_n(x+2)t_n(x)]\left[\prod_{m=1}^{n}[t_m(x+1)]\right] \times [1 - q_n(x-1)[1 - t_n(x)t_n(x-2)]\left[\prod_{m=1}^{n}[t_m(x-1)]\right]\right]\left[\prod_{m=1}^{n+1} t_m(x)\right], \tag{5.1}$$

where

$$t_n(x)=1-S_n(x)\ . \tag{5.2}$$

We now want to average both sides of (5.1) over many clusters, neglecting on the right-hand side of (5.1) correlations between different $S_n(x)$'s [or, what is the same thing, $t_n(x)$'s]. We are interested in the behavior of (5.1) for p near p_c and, in particular, in deducing the value of p_c for this approximation. Recognizing that near p_c $P_n(x)$ is small, we can expand (5.1) keeping only terms that will give rise to terms linear in $P_n(x)$. Furthermore, we can replace all the $q_n(x)$'s on the right-hand side of (5.1) independently by p since no two of them have the same indices and they are all independent. With these simplifications, we have

$$\begin{aligned}\langle t_{n+2}(x)\rangle = f_{n+2}(x) &\cong \langle 1-p(1-\{1-p[1-t_n(x+2)t_n(x)]\}\{1-p[1-t_n(x)t_n(x-2)]\})\rangle \\ &\cong \langle 1-p\{p[2-t_n(x+2)t_n(x)-t_n(x)t_n(x-2)]-p^2[1-t_n(x+2)t_n(x)][1-t_n(x)t_n(x-2)]\}\rangle \\ &= \langle 1-p\{2p-p^2+(p^2-p)[t_n(x+2)t_n(x)+t_n(x)t_n(x-2)]-p^2t_n(x+2)t_n(x)t_n(x-2)\}\rangle \\ &\cong 1-2p^2+p^3+p^2(1-p)[f_n(x+2)f_n(x)+f_n(x)f_n(x-2)]+p^3f_n(x+2)f_n(x)f_n(x-2)\ . \end{aligned} \tag{5.3}$$

The important difference with the zeroth-order approximation appears in the last term on the right-hand side of (5.3): Because the $t_n(x)$'s are idempotent, the last term contains only three factors of t's, and thus three factors of f, and not four as we would have had if we had iterated the deterministic equation (2.9).

To deduce p_c from (5.3), it is sufficient to examine the linear term in the $P_n(x)$'s on the right-hand side of (5.3). We require that the coefficient of the linear term be equal to -1 when $p=p_c$. This yields the condition

$$p^3-4p^2\,|_{p=p_c}=-1\ , \tag{5.4a}$$

or,

$$p_c^3-4p_c^2+1=0\ , \tag{5.4b}$$

from which we find $P_c\cong 0.54$. This value of p_c is closer to the real value of $p_c=1$ than is the value of p_c ($p_c=\frac{1}{2}$) deduced from Eq. (2.9). Note that had there been four factors of f's in the last term on the right-hand side of (5.3), Eq. (5.4) would have been replaced by $4p_c^2=1$, which would have yielded $p_c=\frac{1}{2}$, as we found in Eq. (2.9). Thus, by iterating (2.1) once before taking averages, we have properly accounted for some of the short-range correlations in the stochastic model, and have thus improved our approximation.

Continuation of this procedure will clearly result in improved approximations to the stochastic model. However, the improvements, for example, in the estimate of p_c, seem rather small. Indeed, it is likely that convergence of this procedure to the stochastic result, particularly in the region near p_c, will be rather slow. The reason is that while our procedure allows us to include short-range effects of stochastic noise, it does not take account of long-range effects of noise. To properly compute the behavior of the growth near p_c we need to be able to estimate the long-range effects of stochasticity. This clearly requires the use of renormalization-group techniques, and will be discussed elsewhere.

VI. SUMMARY AND CONCLUSIONS

In this paper we have studied and elucidated a variety of aspects of growth oscillations by examining a number of deterministic algorithms. These algorithms are not only of interest in their own right, but are closely related to certain more realistic stochastic models of growth,[2] and, in fact are mean-field-like approximations to those stochastic models. We have shown that the deterministic models studied in this paper have morphological features as well as growth oscillations which are qualitatively similar to those of the stochastic models to which they are related. Thus, many of the conclusions reached in this study apply also to the stochastic case.

Among the most important insights gleaned from this study, is a better understanding, supplementing the conclusions of Ref. 2, of the origin of growth oscillations. As we have discussed here and in Ref. 2, growth oscillations can generically be expected in kinetically growing structures in which the growth process is discrete (e.g., proceeds by the addition of discrete clumps, or particles of material of well-defined finite size) and in which the growing interface is reasonably narrow. Under these conditions, the dynamics is expected to produce two length scales which in general will be incommensurate. In the case of the simple lattice models discussed here, the average distance grown per time step is in general incommensurate with the lattice spacing, giving rise to the oscillations. In other, nonlattice growth models, oscillations may also be expected. As discussed in Ref. 2, one may expect to see oscillations due to an incommensuration between the particle size and the screening length which controls the average distance over which the aggregating particle penetrates into the structure. Of course, there are additional sources of noise in the nonlattice case and so the oscillations may be considerably more difficult to observe. We are currently studying such nonlattice models.

Many of the specific results of this paper have been derived, for simplicity, in the context of one-dimensional or quasi-one-dimensional models. (This latter term refers to equations which describe growth normal to a facet, so that the structure is translationally invariant in $d-1$ out of d dimensions.) The equations describing these situations have the form of functional iterative maps. In this language we have been able to understand growth oscillations from a different point of view. In terms of iterative maps, we have seen that growth oscillations depend on the existence of competing terms in the map, in a way quite

analogous to the way in which limit cycles depend on competing terms in, for instance, the Feigenbaum map.

For these one-dimensional cases, we have constructed numerical solutions and have shown that growth oscillations exist, and that their behavior is qualitatively the same as that observed in stochastic models. Furthermore, we have been able to solve these equations analytically, by converting a functional iterative map into a hierarchy of an infinite number of single variable linear maps. This hierarchy of maps allows us to construct, in a natural way, an approximation scheme for calculating the effects of growth oscillations. The scheme involves a truncation in the period of the oscillations: In general, growth oscillations give rise to a complicated multiperiodic structure, in which the shorter period oscillations are typically the most pronounced. The approximation scheme discussed in Sec. III includes correctly the effects of oscillations up to a certain wavelength. Higher terms in the approximation include effects of longer-wavelength modulations.

In the context of our deterministic models we were also able to calculate the behavior of the growth near a critical value p_c of the growth parameter. We showed that for $p=p_c$ the density of the cluster falls asymptotically like an inverse power of distance from the origin. This result is the analogue of fractal behavior observed in the analogous stochastic models of growth at the critical value of the growth parameter. We also showed that in quasi-one-dimensional deterministic models of growth there is another critical value p_f of the growth parameter above which there are no growth oscillations. This value p_f represents in these quasi-one-dimensional systems the value of the control parameter at which there is a faceting transition in the analogous case of d-dimensional growth. To be more precise, the analogy is that for $p>p_f$ the quasi-one-dimensional model represents growth normal to a $(d-1)$-dimensional facet in d dimensions. Consistent with the results obtained in the stochastic case, there are no growth oscillations in a direction normal to the facet. In the d-dimensional model, for $p<p_f$ the facet disappears, and growth oscillations appear. Similarly, for $p<p_f$ growth oscillations appear in our quasi-one-dimensional models. However, due to the lack of lateral translational invariance in the d-dimensional case, the quasi-one-dimensional equation does not quantitatively describe d-dimensional growth for $p<p_f$. Nevertheless, because its structure is similar to that of the full d-dimensional growth near a $(d-1)$-dimensional faceting transition, the quasi-one-dimensional equation does correctly describe the qualitative behavior of the d-dimensional case, including the existence of the faceting transition and the presence (absence) of growth oscillations for $p<(>)p_f$. (Of course, if we consider growth in d dimensions starting from a $d-1$ dimensional hyperplane, then our quasi-one-dimensional equation will quantitatively describe the growth for all values of p.)

We were also able to elucidate the multiperiodic nature of the growth oscillations and were able to provide a simple procedure for estimating the fundamental wavelength of the oscillations. Nearly all of the techniques and conclusions which we derived in the context of one dimensional and quasi-one-dimensional growth can be applied, with some modifications, to higher-dimensional systems.

Finally, we described a sequence of approximations, the lowest order of which are the deterministic models studied in this paper, and which approach successively closer to the stochastic models. We showed, in particular, a small improvement in the estimate for p_c by going from our deterministic model to the next order of approximation in one particularly simple case.

While the study of growth oscillations we have presented here is a useful beginning, there are a number of very intriguing questions that require further work. There are two issues that are particularly interesting and important. First, it is important to understand more precisely, the stability of growth oscillations to noise. In a previous paper,[1,2] we presented an argument relating the persistence of growth oscillations to the roughening exponent of the growing interface. While this argument is appealing, a more complete and precise treatment of the stability of growth oscillations to noise is clearly desirable. Second, it is important to be able to compute the effects of stochasticity near p_c more reliably. We have already showed that our deterministic model has a power-law-behaved density at $p=p_c$. However, to realistically calculate kinetic fractal growth, requires that we be able to accurately compute the long range effects of stochasticity, as stated at the end of Sec. V. It is likely that the conceptual framework we have developed in connection with our study of growth oscillations will be of great use in trying to calculate properties of kinetic fractal growth.

ACKNOWLEDGMENTS

We are grateful to S. Alexander, G. Grinstein, D. Kessler, and L. Sander for interesting discussions. R. S. thanks the Hebrew University of Jerusalem and the Weizmann Institute of Science where part of this work was carried out, for their hospitality and support. This work was supported by the U. S. Department of Energy under Grant No. DE-FG02-85ER45189.

[1]Z. Cheng and R. Savit, J. Phys. A (Lett.) **19**, L973 (1986).

[2]R. Baiod, Z. Cheng, and R. Savit, Phys. Rev. B **34**, 7764 (1986).

[3]Z. Cheng, L. Jacobs, D. Kessler, and R. Savit (unpublished).

[4]R. Savit, and R. Ziff, Phys. Rev. Lett. **55**, 2515 (1985); R. Ziff, R. Savit, and R. Baiod (unpublished).

[5]See, for example, S. R. Broadbent and J. M. Hammersley, Proc. Cambridge Philos. Soc. **53**, 629 (1957); P. L. Leath, Phys. Rev. B **14**, 5046 (1976); Z. Alexandrowicz, Phys. Lett. **80A**, 284 (1980).

[6]Actually, due to a detail of the growth algorithm, $P_n(x)\equiv 0$ for x odd (even) if n is even (odd). In these figures in which we indicate $P_n(x)$ for a given n, we only connect the nonzero values of $P_n(x)$ with solid lines. This feature of the growth algorithm is not important for our present purposes, and will be discussed in more detail below.

[7]Note, however, that in a certain sense $p\to 1$ may herald chaotic behavior since the "limit cycles" become longer in period. Furthermore, in the model studied in Sec. IV this limit is reached as $p\to P_f<1$. See below for more details.

[8]M. J. Feigenbaum, J. Stat. Phys. **19**, 25 (1978); **21**, 699 (1979).

[9]Do not confuse the fixed point for Eq. (4.2) as $n \to \infty$ with the terminology we have used to describe the behavior of the functional maps such as (2.9) or (2.13). We have described the behavior of (2.9) or (2.13) in the region in which there are growth oscillations as limit cycle behavior. But even in these regions Eqs. (4.2) have fixed-point behavior as $n \to \infty$ for fixed L. See below for more details.